HIGGS BOSON RADIATION IN ARBITRARILY POLARIZED ELECTRON-POSITRON COLLISIONS

M.Sh. GOJAYEV
23, acad. Z. Khalilov, Baku State University,
Baku, Azerbaijan, AZ1148
m_qocayev@mail.ru

Recently, the ATLAS and CMS collaborations at LHC announced Higgs boson like particle with mass around 125 GeV. To explore its physical properties, different observables are needed to be measured precisely at the various processes with the Higgs boson. In this paper in the framework of the Standard Model the Higgs boson and a heavy fermion pair production process in electron-positron collisions in considered: $e^-e^+ \to H f\bar{f}$, here $f\bar{f}$ – is the lepton pair ($\tau^-\tau^+$) or quark pair ($b\bar{b}$, $t\bar{t}$). The mechanism of Higgs boson radiation by a heavy fermion pair is investigated in detail. Taking into account the arbitrarily (longitudinal and transverse) polarizations of the electron-positron pair and the longitudinal polarizations of the fermion pair, analytical expressions for the differential and integral cross sections are obtained. The left-right and transverse spin asymmetries, as well as the degree of longitudinal polarizations of the fermion are determined. At the energy of the electron-positron pair $\sqrt{s}$ =1 TeV, the dependence of the effective cross section and asymmetries on the energies and angles of departure was studied. The possibility of measuring the coupling constant of the Higgs boson with a $t\bar{t}$ -quark pair is discussed.

Keywords: Standard Model, Minimal Supersymmetric Standard Model, electron-positron pair, Higgs boson, decay width, coupling constant.
PACS: 12.15-y, 12.15 Mm, 14.70 Hp, 14.80 Bn.

1. INTRODUCTION

The Standard model (SM), based on the local gauge theory with a symmetry group $SU_C(3)\times SU_L(2)\times U_Y(1)$, satisfactorily describes the physics of strong, electromagnetic and weak interactions between quarks, leptons, and gauge bosons [1-5]. In elementary particle physics, not a single experiment has yet been observed, the results of which are not consistent with the SM. Recently opened the missing bricks in the building SM. These is the scalar Higgs boson, discoveries by the ATLAS and CMS collaborations [6, 7] (see also reviews [8-10]) at the Large Hadron Collider (LHC) at CERN. The discovery of the Higgs boson experimentally confirmed the theoretically predicted mechanism for the generation of masses of fundamental particles – the mechanism of spontaneous breaking of the Brout-Englert-Higgs symmetry [11–14].

In experiments conducted in the LHC, the main properties of this particle were established. The Higgs boson is a scalar particle with spin zero, positive parity, nonzero vacuum value, mass about 125 GeV, interacting with $W^{\pm}$- and Z^0-bosons with a coupling constant proportional to their masses. With the discovery of the Higgs boson H, the SM has entered a new stage in the study of the properties of the fundamental interactions of elementary particles. An accurate measurement of all the coupling constants of this particle with fundamental fermions can be an argument in favor of or a counterbalance to the fact that it is in fact a Higgs boson of the SM. In this connection, interest in various channels of the Higgs boson production and decay has greatly increased [1, 15–29].

Determining the physical characteristics of the Higgs boson H is the main task of the LHC, as well as future high-energy electron-positron colliders. Note that the collision of electrons and positrons at high energies is an effective method for studying the mechanisms of interaction of elementary particles. This is mainly due to the following two circumstances. First, the interaction of electrons and positrons is described by the electroweak Weinberg-Salam theory; therefore, the results obtained are well interpretable. Secondly, since electrons and positrons do not participate in strong interactions, the background conditions of the experiments are significantly improved compared with the studies conducted with hadron beams. The latter circumstance is especially significant when studying processes with small cross sections. We only note that experiments carried out with electron-positron beams at LEP and SLC acceleration centers up to energies of $\sqrt{s} = 209$ GeV in the center-of-mass system played an essential role for precision testing of the SM [1, 2].

At present, the construction of a new generation of electron-positron colliders ILC (International Linear Collider), CLIC (Compact Linear Collider), FCC-ee (Future Circular Collider), CEPC (Circular Electron Positron Collider) [23, 30] has been designed. In the future, these colliders will allow us to study the physical properties of the standard Higgs boson.

In recent works [16, 27], we have investigated the processes of production of the Higgs boson and light fermion pair in arbitrarily polarized electron-positron collisions. The associated production of the Higgs boson and the heavy fermion pair was first considered in [31]. Here authors consider the electromagnetic mechanism of the production of a heavy fermion pair and the Higgs boson radiation from the fermion line $e^- + e^+ \to (\gamma^*) \to f + \bar{f} + H$. In [32] (see also [33]), in the framework of the SM, the production of the Higgs

131, H. Javid ave., AZ-1143, Baku
ANAS, G.M. Abdullayev Institute of Physics
E-mail: jophphysics@gmail.com

boson H and a heavy $t\bar{t}$-quark pair was considered $e^- + e^+ \to (\gamma^*; Z^*) \to H + t + \bar{t}$. Here, a cross section is obtained, integrated over the angles of emission of particles and characterizing the distribution of the $t\bar{t}$-quark pair by energy. In a recent paper [34, 35], we investigated the electromagnetic mechanism of the process $e^- + e^+ \to (\gamma^*) \to H + f + \bar{f}$ with allowance for arbitrary polarizations of the electron-positron pair and the helicities of heavy fermions.

In the present work, we studied the associated production of the standard Higgs boson H and a heavy fermion pair in arbitrarily polarized electron-positron collisions in the framework of the SM:

$$e^- + e^+ \to (\gamma^*; Z^*) \to H + f + \bar{f} \qquad (1)$$

where $f\bar{f}$ –may be a lepton ($\tau^-\tau^+$) or quark ($b\bar{b}$, $t\bar{t}$) pair. The differential and integral cross sections of the process are calculated taking into account the polarizations of the particles. The possibility of measuring the fundamental constant of the SM, the Higgs boson coupling constant of with a heavy fermion pair, is discussed, which is very important for verifying the Higgs sector of the SM.

2. DIFFERENTIAL CROSS SECTION OF REACTION $e^-e^+ \to Hf\bar{f}$

In the SM process (1) is described by two types of Feynman diagrams, shown in fig. 1, where 4-momenta of the particles are written in parentheses. Diagrams a) and b) correspond to the Higgs boson radiation by a heavy fermion pair, and c) describes the Higgs boson radiation by the intermediate vector Z^0-boson.

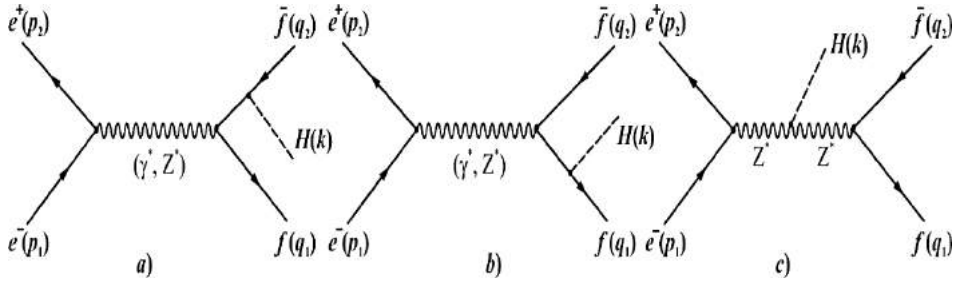

Fig. 1. Feynman diagrams for the associated production of Higgs boson with a fermion pair.

Within the framework of the SM, the matrix element corresponding to diagrams a) and b) can be written as (note that diagram c) was studied in detail in a recent paper [16], which is why it is not considered here)

$$M_{i\to f} = M^{(\gamma)}_{i\to f} + M^{(Z)}_{i\to f}, \qquad (2)$$

$$M^{(\gamma)}_{i\to f} = \frac{ie^2 Q_e Q_f}{s} g_{Hff} \cdot \ell^{(\gamma)}_{\mu} \cdot J^{(\gamma)}_{\mu}, \qquad (3)$$

$$M^{(Z)}_{i\to f} = \frac{ie^2}{s - M_Z^2} g_{Hff} \cdot \ell^{(Z)}_{\mu} \cdot J^{(Z)}_{\mu}. \qquad (4)$$

Here $Q_e = -1$ – is the electric charge of an electron in units e;

$$\ell^{(\gamma)}_{\mu} = \bar{\upsilon}_e(p_2)\gamma_\mu u_e(p_1),$$

$$J^{(\gamma)}_{\mu} = \bar{u}_f(q_1)\left[\frac{\hat{q}_1 + \hat{k} + m_f}{(q_1+k)^2 - m_f^2}\gamma_\mu - \gamma_\mu \frac{\hat{q}_2 + \hat{k} - m_f}{(q_2+k)^2 - m_f^2}\right]\upsilon_f(q_2), \qquad (5)$$

$$\left.\begin{aligned} \ell^{(Z)}_{\mu} &= \bar{\upsilon}_e(p_2)\gamma_\mu[g_V(e) + \gamma_5 g_A(e)]u_e(p_1), \\ J^{(Z)}_{\mu} &= \bar{u}_f(q_1)\left\{\frac{\hat{q}_1 + \hat{k} + m_f}{(q_1+k)^2 - m_f^2}\gamma_\mu[g_V(f) + \gamma_5 g_A(f)] - \gamma_\mu[g_V(f) + \right. \\ &\left. + \gamma_5 g_A(f)]\frac{\hat{q}_2 + \hat{k} - m_f}{(q_2+k)^2 - m_f^2}\right\}\upsilon_f(q_2), \end{aligned}\right\} \qquad (6)$$

– electromagnetic (weak) currents of the electron-

positron and heavy fermion pair; $s = p^2 = (p_1 + p_2)^2$ – the square of the total energy e^-e^+-pairs in the center of mass system, m_f and Q_f – the mass and electric charge of the fermion f, g_{Hff} – the Higgs boson coupling constant with a heavy fermion pair, M_Z – the mass of a Z^0-boson, $g_V(e)$ and $g_A(e)$ ($g_V(f)$ and $g_A(f)$) – the vector and axial-vector coupling constants of the electron (fermion) with Z^0-boson. In SM, these coupling constants are defined by the expressions

$$\left.\begin{aligned} g_V(e) &= \frac{-\frac{1}{2} + 2x_W}{2\sqrt{x_W(1-x_W)}}, \qquad g_A(e) = \frac{-\frac{1}{2}}{2\sqrt{x_W(1-x_W)}}, \\ g_V(f) &= \frac{I_3(f) - 2Q_f x_W}{2\sqrt{x_W(1-x_W)}}, \quad g_A(f) = \frac{I_3(f)}{2\sqrt{x_W(1-x_W)}}, \end{aligned}\right\} \tag{7}$$

where $x_W = \sin^2\theta_W$ – is the Weinberg parameter, $I_3(f) = \pm 1/2$ – is the third projection of the weak isospin of the fermion f.

The square of the matrix element (2) is expressed by the formula

$$\left|M_{i\to f}\right|^2 = \frac{e^4}{s^2} g_{Hff}^2 [Q_e^2 Q_f^2 L_{\mu\nu}^{(\gamma)} \cdot H_{\mu\nu}^{(\gamma)} + 2Q_e Q_f X_Z L_{\mu\nu}^{(i)} \cdot H_{\mu\nu}^{(i)} + X_Z^2 L_{\mu\nu}^{(Z)} \cdot H_{\mu\nu}^{(Z)}] \cdot \tag{8}$$

Here $X_Z = \left(1 - \frac{M_Z^2}{s}\right)^{-1}$, $L_{\mu\nu}^{(\gamma)}$ ($H_{\mu\nu}^{(\gamma)}$), $L_{\mu\nu}^{(Z)}$ ($H_{\mu\nu}^{(Z)}$) and $L_{\mu\nu}^{(i)}$ ($H_{\mu\nu}^{(i)}$) are the electromagnetic, weak, and interference tensors of the electron-positron (heavy fermion) pair. Due to the conservation of electron-positron currents $\ell_\mu^{(\gamma)}$ and $\ell_\mu^{(Z)}$, the contribution to the cross section is made only by the spatial components of the tensors

$$L_{\mu\nu}^{(a)} \cdot H_{\mu\nu}^{(a)} = L_{mr}^{(a)} \cdot H_{mr}^{(a)} \qquad (m, r = 1,2,3;\ a = \gamma, i, Z).$$

Electron-positron tensors $L_{mr}^{(a)}$ are easily calculated on the basis of currents $\ell_\mu^{(\gamma)}$ and $\ell_\mu^{(Z)}$, in the case of arbitrarily polarized e^-e^+-pairs, they have the following structure [36, 37]:

$$\begin{aligned} L_{mr}^{(\gamma)} &= \ell_m^{(\gamma)} \ell_r^{*(\gamma)} = \frac{s}{2}[(1-\lambda_1\lambda_2)(\delta_{mr} - N_m N_r) + (\lambda_2 - \lambda_1) i\varepsilon_{mrs} N_s + \\ &+ (\vec{\eta}_1\vec{\eta}_2)(\delta_{mr} - N_m N_r) - \eta_{1m}\eta_{2r} - \eta_{1r}\eta_{2m}], \\ L_{mr}^{(i)} &= \ell_m^{(\gamma)} \ell_r^{*(Z)} = g_V(e) L_{mr}^{(\gamma)} + \frac{s}{2} \cdot g_A(e)[(\lambda_2 - \lambda_1)(\delta_{mr} - N_m N_r) + (1-\lambda_1\lambda_2) i\varepsilon_{mrs} N_s], \\ L_{mr}^{(Z)} &= \ell_m^{(Z)} \ell_r^{*(Z)} = [g_V^2(e) + g_A^2(e)] L_{mr}^{(\gamma)} + \frac{s}{2} \cdot 2 g_V(e) g_A(e)[(\lambda_2 - \lambda_1)(\delta_{mr} - N_m N_r) + \\ &+ (1-\lambda_1\lambda_2) i\varepsilon_{mrs} N_s] - s \cdot g_A^2(e)[(\vec{\eta}_1\vec{\eta}_2)(\delta_{mr} - N_m N_r) - \eta_{1m}\eta_{2r} - \eta_{1r}\eta_{2m}], \end{aligned} \tag{9}$$

where λ_1 and λ_2 ($\vec{\eta}_1$ and $\vec{\eta}_2$) are the helicities (the transverse components of the spin vectors) of the electron and positron, $\vec{N}$ –is a unit vector directed along the electron momentum.

From the expressions of tensors (9), it follows that the longitudinally polarized electron and positron must have opposite helicities $\lambda_1 = -\lambda_2 = \pm 1$ (the left electron, and the right positron – $e_L^- e_R^+$ or the right electron, and the left positron – $e_R^- e_L^+$). This is due to the preservation of the total momentum in the transitions $e^- + e^+ \to \gamma^*$ and $e^- + e^+ \to Z^*$.

As for the fermionic tensors of a heavy fermion pair $H_{mr}^{(a)}$, we note that in the general case they have a cumbersome expressions, therefore they are not given here. However, at high energies of colliding particles ($\sqrt{s} \geq 1$ TeV), the rations m_f^2/s and M_H^2/s can be neglected (for example, when $\sqrt{s} = 1$ TeV for a heavy t-quark this ratio is $\left(\frac{173.2}{1000}\right)^2 = 0.03 << 1$). Then for the tensors $H_{mr}^{(a)}$ we have the following expressions (we assume that the heavy fermion pair is polarized longitudinally):

$$
\left.
\begin{aligned}
H_{mr}^{(\gamma)} &= J_m^{(\gamma)} J_r^{*(\gamma)} = \frac{x_H^2}{2(1-x_1)(1-x_2)}[(1+h_1h_2)(\delta_{mr}-n_m n_r)+(h_1+h_2)i\varepsilon_{mrq}n_q],\\
H_{mr}^{(i)} &= J_m^{(\gamma)} J_r^{*(Z)} =\\
&= g_V(f)H_{mr}^{(\gamma)} + \frac{1}{4}g_A(f)(1+h_1h_2)\cdot x_H \cdot i\varepsilon_{mrq}\left[\frac{x_2}{1-x_2}(n_{2q}-n_q)-\frac{x_1}{1-x_1}(n_{1q}-n_q)\right]+\\
&+\frac{1}{4}g_A(f)(h_1+h_2)\left\{\frac{1}{1-x_2}\left[x_H x_2(n_m n_{2r}+n_r n_{2m})+2(1-x_1)\delta_{mr}\right]-\right.\\
&\left.-\frac{1}{1-x_1}\left[x_H x_1(n_m n_{1r}+n_r n_{1m})+2(1-x_2)\delta_{mr}\right]\right\}.\\
H_{mr}^{(Z)} &= J_m^{(Z)} J_r^{*(Z)} = [g_V^2(f)+g_A^2(f)]H_{mr}^{(\gamma)} - g_A^2(f)(1+h_1h_2)(1+x_H)(\delta_{mr}-n_m n_r)-\\
&-\frac{1}{2}\cdot g_A^2(f)(h_1+h_2)x_H i\varepsilon_{mrq}\left[\frac{x_2}{1-x_1}(n_{2q}-n_q)-\frac{x_1}{1-x_2}(n_{1q}-n_q)\right]+\\
&+\frac{1}{2}g_V(f)g_A(f)(1+h_1h_2)x_H i\varepsilon_{mrq}\left[\frac{x_2}{1-x_2}(n_{2q}-n_q)-\frac{x_1}{1-x_1}(n_{1q}-n_q)\right]+\\
&+\frac{1}{2}g_V(f)g_A(f)(h_1+h_2)\left\{\frac{1}{1-x_2}[x_H x_2(n_m n_{2r}+n_r n_{2m})+2(1-x_1)\delta_{mr}]-\right.\\
&\left.-\frac{1}{1-x_1}[x_H x_1(n_m n_{1r}+n_r n_{1m})+2(1-x_2)\delta_{mr}]\right\}.
\end{aligned}
\right\} \qquad (10)
$$

Here h_1 and h_2 – are the helicities of the fermion and antifermion, $x_1 = 2E_1/\sqrt{s}$, $x_2 = 2E_2/\sqrt{s}$ and $x_H = 2E_H/\sqrt{s} = 2 - x_1 - x_2$ – are the scaling energies of the fermion, antifermion and Higgs boson, respectively, $\vec{n}$, $\vec{n}_1$ and $\vec{n}_2$ – are the unit vectors along the Higgs boson, fermion and antifermion momentums.

As follows from the tensors $H_{mr}^{(a)}$, the helicity of the fermion and the antifermion, in contrast to the helicity of the electron-positron pair, must be the same $h_1 = h_2 = \pm 1$ ($f_R\bar{f}_R$ or $f_L\bar{f}_L$).

This is due to the conservation of the total momentum at the Higgs boson emission by the fermion or antifermion ($f \to f + H$, $\bar{f} \to \bar{f} + H$). We note that when the Higgs boson is emitted by the vector Z-boson, due to the conservation of the total momentum in the transition $Z^* \to f + \bar{f}$, the fermion and the antifermion must have opposite helicities ($h_1 = -h_2 = \pm 1$, $f_L\bar{f}_R$ and $f_R\bar{f}_L$). Consequently, it is possible to separate the contributions of the diagrams a) and b) from the contribution of the diagram c) along the helicities of the fermion and the antifermion.

We use a coordinate system in which the OXZ plane coincides with the particle production plane $\vec{q}_1 + \vec{q}_2 + \vec{k} = 0$, and we introduce angles θ, χ and φ, where θ – is the polar angle between the Z axis and the direction of the electron beam, χ – is the azimuth angle between the production plane and the plane defined by the Z axis and the electron beam, φ – the azimuth angle between the planes of production and transverse polarization of the electron. In this coordinate system, the angular distribution of particles over the angles φ, θ and χ in the case of arbitrarily polarized electron-positron and longitudinally polarized fermion-antifermion pairs is given by:

$$
\frac{d^5\sigma}{d\varphi d\chi d(\cos\theta)dx_1dx_2} = \frac{\alpha_{\mathrm{QED}}^2 N_C}{256\pi^3 s^2} g_{Hff}^2 [Q_e^2 Q_f^2 L_{mr}^{(\gamma)}\cdot H_{mr}^{(\gamma)} + 2Q_eQ_f X_Z L_{mr}^{(i)}\cdot H_{mr}^{(i)} + X_Z^2 L_{mr}^{(Z)}\cdot H_{mr}^{(Z)}], \qquad (11)
$$

where N_C – is the color factor (in the case of the production of a lepton pair $\tau^-\tau^+$ $N_C = 1$, and in the case of the production of a quark pair $b\bar{b}$ or $t\bar{t}$ $N_C = 3$).

3. ANGULAR CORRELATIONS IN THE PROCESS $e^-e^+ \to Hf\bar{f}$

We introduce the so-called correlation functions $\sigma_n\,(n = 1 \div 9)$, by means of the relations

$$\left.\begin{aligned}
&\sigma_1 = H_{11} + H_{22}, \qquad \sigma_2 = \frac{1}{2}(H_{22} - H_{11}), \quad \sigma_3 = H_{33},\\
&\sigma_4 = \frac{1}{2}(H_{13} + H_{31}), \quad \sigma_5 = \frac{1}{2}(H_{23} + H_{32}), \quad \sigma_6 = \frac{1}{2}(H_{12} + H_{21}),\\
&\sigma_7 = i(H_{12} - H_{21}), \quad \sigma_8 = \frac{i}{2}(H_{23} - H_{32}), \quad \sigma_9 = \frac{i}{2}(H_{31} - H_{13}).
\end{aligned}\right\} \tag{12}$$

Then the product of the electron-positron and fermionic tensors can be represented as:

$$L_{mr} \cdot H_{mr} = \frac{1}{2}(L_{11} + L_{22}) \cdot \sigma_1 + (L_{22} - L_{11}) \cdot \sigma_2 + L_{33} \cdot \sigma_3 + (L_{13} + L_{31}) \cdot \sigma_4 + (L_{23} +$$

$$+ L_{32}) \cdot \sigma_5 + (L_{12} + L_{21}) \cdot \sigma_6 - \frac{i}{2}(L_{12} - L_{21}) \cdot \sigma_7 - i(L_{23} - L_{32}) \cdot \sigma_8 - i(L_{31} - L_{31}) \cdot \sigma_9. \tag{13}$$

For the distribution of particles over the angles θ and χ in the reaction (1) the expression is obtained

$$\frac{d^4\sigma}{d\chi d(\cos\theta) dx_1 dx_2} = \frac{\alpha_{\text{QED}}^2 N_C}{128\pi^2 s} g_{Hff}^2 [G_A \cdot \sigma_A + G_B \cdot \sigma_B + G_C \cdot \sigma_C]. \tag{14}$$

The notation is entered here

$$\left.\begin{aligned}
&G_A = Q_e^2 Q_f^2 + 2Q_e Q_f g_V(e) g_V(f) X_Z + [g_V^2(e) + g_A^2(e)][g_V^2(f) + g_A^2(f)] X_Z^2,\\
&G_B = 2g_A(e) g_A(f)[Q_e Q_f + 2g_V(e) g_V(f) X_Z] X_Z,\\
&G_C = [g_V^2(e) + g_A^2(e)] g_A^2(f) X_Z^2
\end{aligned}\right\} \tag{15}$$

and functions

$$\left.\begin{aligned}
&\sigma_A = \frac{1}{2}(1 + \cos^2\theta) \cdot \sigma_1 + \sin^2\theta(\cos 2\chi \cdot \sigma_2 + \sigma_3 + \sin 2\chi \cdot \sigma_4) + \sin 2\theta(\sin\chi \cdot \sigma_5 + \cos\chi \cdot \sigma_6),\\
&\sigma_B = \cos\theta \cdot \sigma_7 + 2\sin\theta(\cos\chi \cdot \sigma_8 + \sin\chi \cdot \sigma_9),\\
&\sigma_C = \frac{1}{2}(1 + \cos^2\theta) \cdot \sigma_1' + \sin^2\theta(\cos 2\chi \cdot \sigma_2' + \sigma_3' + \sin 2\chi \cdot \sigma_4') + + \sin 2\theta(\sin\chi \cdot \sigma_5' + \cos\chi \cdot \sigma_6').
\end{aligned}\right\} \tag{16}$$

Correlation functions σ_n and σ_n', entering in (16), depend on scaling energies x_1 and x_2 ($x_H = 2 - x_1 - x_2$) and they are easily determined on the basis of fermionic tensors (10):

$$\left.\begin{aligned}
&\sigma_1 = \frac{2x_H^2}{(1-x_1)(1-x_2)}(2 - n_x^2), && \sigma_2 = \frac{x_H^2}{(1-x_1)(1-x_2)} n_x^2,\\
&\sigma_3 = \frac{2x_H^2}{(1-x_1)(1-x_2)}(1 - n_z^2), && \sigma_4 = -\frac{2x_H^2}{(1-x_1)(1-x_2)} \cdot n_x n_z,\\
&\sigma_7 = 2x_H\left[\frac{x_2}{1-x_2}(n_z - n_{2z}) - \frac{x_1}{1-x_1}(n_z - n_{1z})\right], && \sigma_8 = x_H\left[\frac{x_2}{1-x_2}(n_x - n_{2x}) - \frac{x_1}{1-x_1}(n_x - n_{1x})\right],\\
&\sigma_5 = \sigma_6 = \sigma_9 = 0, && \sigma_1' = -4(1 + x_H)(2 - n_x^2), \quad \sigma_2' = -2(1 + x_H) n_x^2,\\
&\sigma_5' = \sigma_6' = 0. && \sigma_3' = -4(1 + x_H)(1 - n_z^2), \quad \sigma_4' = 4(1 + x_H) n_x n_z.
\end{aligned}\right\} \tag{17}$$

As can be seen, due to the orthogonality of the Y axis to the particle production plane, the correlation functions σ_5, σ_6, σ_9, σ_5' and σ_6' vanish.

In the case of massless fermions and Higgs boson, the distribution of particles in the Dalitz diagram is determined by the laws of conservation of energy and momentum:

$$x_1 + x_2 + x_H = 2, \qquad x_1\vec{n}_1 + x_2\vec{n}_2 + x_H\vec{n} = 0.$$

The boundaries of the allowed region are given by the equations

$$x_k = \left| x_i \pm x_j \right| \quad (i \neq j \neq k).$$

The lines $x_1 = x_2$, $x_1 = x_H$ and $x_2 = x_H$ divide the Dalitz diagram into six different areas. In the region of $(i;\ j)$ the scaling energies of the particles x_i and x_j satisfy the conditions

$$x_i \geq x_j \geq x_k \quad (i \neq j \neq k).$$

We can direct the axis Z along the most energetic particle and choose an axis X so that the x projection of the momentum of the second more energetic particle becomes positive. Then the following areas of the Dalitz diagram are obtained.

Ia (3; 1). The axis Z is directed along the momentum of the more energetic Higgs boson, and the momentum of the second energetic fermion has a positive x-projection (see fig. 2a)

$$\vec{n} = (0,\ 0,\ 1), \quad \vec{n}_1 = (s_{31},\ 0,\ c_{31}), \quad \vec{n}_2 = (-s_{32},\ 0,\ c_{32}).$$

Similarly, we have the following areas:

Ib(3; 2): $\vec{n}=(0,\,0,\,1),\ \vec{n}_1=(-s_{31},\,0,\,c_{31}),\ \vec{n}_2=(s_{32},\,0,\,c_{32});$
IIa(1; 2): $\vec{n}_1=(0,\,0,\,1),\ \vec{n}_2=(s_{12},\,0,\,c_{12}),\ \vec{n}=(-s_{13},\,0,\,c_{13});$
IIb(1; 3): $\vec{n}_1=(0,\,0,\,1),\ \vec{n}_2=(-s_{12},\,0,\,c_{12}),\ \vec{n}=(s_{13},\,0,\,c_{13});$
IIIa(2; 1): $\vec{n}_2=(0,\,0,\,1),\ \vec{n}_1=(s_{21},\,0,\,c_{21}),\ \vec{n}=(-s_{23},\,0,\,c_{23});$
IIIb(2; 3): $\vec{n}_2=(0,\,0,\,1),\ \vec{n}_1=(-s_{21},\,0,\,c_{21}),\ \vec{n}=(s_{23},\,0,\,c_{23}).$

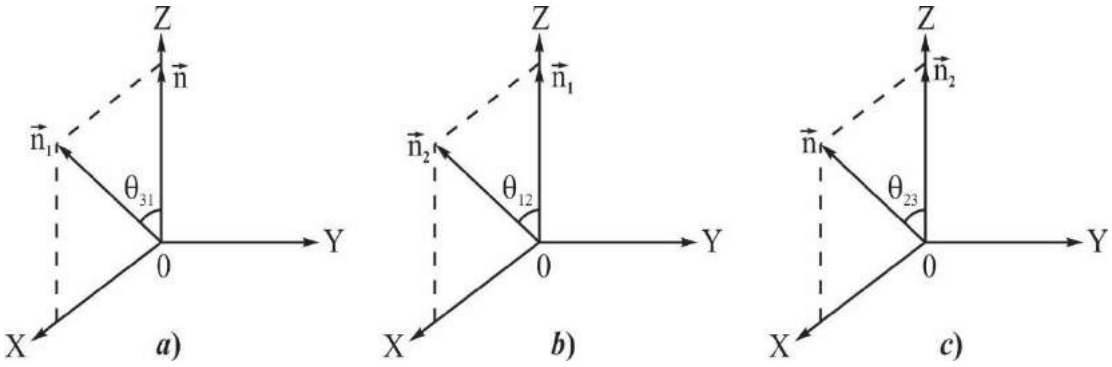

Fig. 2. The coordinate systems Ia, IIa and IIIb.

Here we have used the notation $s_{ij}=\sin\theta_{ij}$ and $c_{ij}=\cos\theta_{ij}$, where θ_{ij} – the angle between the directions of the momenta of the particles i and j. These angles depend on the scaling energies of the particles

$$\left.\begin{aligned}\sin\theta_{ij}&=\frac{2\sqrt{(1-x_1)(1-x_2)(1-x_H)}}{x_i x_j},\\ \cos\theta_{ij}&=1-\frac{2(x_i+x_j-1)}{x_i x_j}.\end{aligned}\right\}\qquad(18)$$

Using these expressions, we can easily determine the correlation functions in each area of the Dalitz diagram. Here we present the correlation functions in the coordinate system Ia (Ib), where the momentum of the more energetic Higgs boson is directed along the axis Z, and the second energetic fermion (antifermion) in the production plane has a positive momentum projection $q_{1x}>0$ ($q_{2x}>0$):

$$\left.\begin{aligned}&\sigma_1=\frac{4x_H^2}{(1-x_1)(1-x_2)}=4\left(2+\frac{1-x_1}{1-x_2}+\frac{1-x_2}{1-x_1}\right),\\ &\sigma_7=2x_H\left[\frac{x_2}{1-x_2}(1-c_{32})-\frac{x_1}{1-x_1}(1-c_{31})\right],\\ &\sigma_1'=-8(1+x_H),\ \sigma_2=\sigma_3=\sigma_4=\sigma_8=\sigma_2'=\sigma_3'=\sigma_4'=0.\end{aligned}\right\}\qquad(19)$$

The expressions for the correlation functions in the coordinate systems IIa, b and IIIa, b are given in the Appendix.

The distribution of particles over the angles θ and χ present in the form:

$$\frac{d^4\sigma}{d\chi d(\cos\theta)dx_1dx_2}=\frac{\alpha_{\rm QED}^2N_C}{128\pi^2 s}g_{Hff}^2G_A(\sigma_1+2\sigma_3)(1+\alpha_0)[1+\alpha_1\cos^2\theta+$$
$$+\alpha_2\sin^2\theta\cos2\chi+\alpha_4\sin^2\theta\sin2\chi+\alpha_7\cos\theta+\alpha_8\sin\theta\cos\chi],\qquad(20)$$

where the coefficients of the angular distributions of particles are determined by the expressions

$$\left.\begin{aligned}&\alpha_0=\frac{G_C}{G_A}\cdot\frac{\sigma_1'+2\sigma_3'}{\sigma_1+2\sigma_3},\qquad \alpha_1=\frac{1}{1+\alpha_0}\cdot\left[\frac{\sigma_1-2\sigma_3}{\sigma_1+2\sigma_3}+\frac{G_C}{G_A}\cdot\frac{\sigma_1'-2\sigma_3'}{\sigma_1+2\sigma_3}\right],\\ &\alpha_2=\frac{1}{1+\alpha_0}\cdot\left[\frac{2\sigma_2}{\sigma_1+2\sigma_3}+\frac{G_C}{G_A}\cdot\frac{2\sigma_2'}{\sigma_1+2\sigma_3}\right],\quad \alpha_4=\frac{1}{1+\alpha_0}\cdot\left[\frac{2\sigma_4}{\sigma_1+2\sigma_3}+\frac{G_C}{G_A}\cdot\frac{2\sigma_4'}{\sigma_1+2\sigma_3}\right],\\ &\alpha_7=\frac{1}{1+\alpha_0}\cdot\frac{G_B}{G_A}\cdot\frac{2\sigma_7}{\sigma_1+2\sigma_3},\qquad \alpha_8=\frac{1}{1+\alpha_0}\cdot\frac{G_B}{G_A}\cdot\frac{4\sigma_8}{\sigma_1+2\sigma_3}.\end{aligned}\right\}\qquad(21)$$

Let us estimate the coefficients of the angular distributions α_k $(k = 1, 2, 4, 7, 8)$ in the coordinate system IIIb, where the momentum of the more energetic antifermion is directed along the axis Z, and the momentum of the second energetic Higgs boson in the production plane has a positive x-projection $k_x > 0$ (see fig. 2c). Using the expressions of the correlation functions given in the Appendix, for these coefficients we have the expressions:

$$\alpha_0 = -\frac{G_C}{G_A}\cdot\frac{2}{x_H^2}(1+x_H)(1-x_1)(1-x_2), \quad \alpha_1 = \frac{3c_{23}^2-1}{3-c_{23}^2}\cdot\frac{1-\alpha_0}{1+\alpha_0},$$

$$\alpha_2 = \frac{s_{23}^2}{3-c_{23}^2}\cdot\frac{1-\alpha_0}{1+\alpha_0}, \qquad \alpha_4 = -\frac{2s_{23}c_{23}}{3-c_{23}^2}\cdot\frac{1-\alpha_0}{1+\alpha_0},$$

$$\alpha_7 = \frac{G_B}{G_A}\frac{1}{1+\alpha_0}\frac{2[x_2(1-x_1)(c_{23}-1)-x_1(1-x_2)(c_{23}-c_{21})]}{x_H(3-c_{23}^2)}, \tag{22}$$

$$\alpha_8 = \frac{G_B}{G_A}\frac{1}{1+\alpha_0}\frac{2[x_2(1-x_1)s_{23}-x_1(1-x_2)(s_{23}+s_{21})]}{x_H(3-c_{23}^2)}.$$

In fig. 3 shows the dependence of the coefficients on a variable x_2 with a fixed scaling energy $x_1 = 0.9$ in the process $e^- + e^+ \to H + t + \bar{t}$. Here and in further calculations, the energy of electron-positron beams is assumed $\sqrt{s}$ = 1 TeV, mass of Z^0-boson M_Z = 91.1875 GeV, mass of t-quark m_t = 173.2 GeV, Weinberg parameter x_W = 0.232. As you can see, the coefficient α_1 (α_7, α_8) is negative and decreases (increases) with increasing energy x_2. The coefficient of the angular distribution α_2 is positive and slowly increase with increasing variable x_2. The angular distribution coefficient α_4 at the beginning of the energy spectrum is negative, it increases with increasing x_2 and at the end of the energy spectrum becomes positive.

4. LEFT-RIGHT AND TRANSVERSE SPIN ASYMMETRIES AND THE DEGREE OF LONGITUDINAL POLARIZATION OF THE FERMION

When electron-positron pair a longitudinally polarized the differential cross section of reaction (1), integrated over the angles θ and χ, can be represented as:

$$\frac{d^2\sigma(\lambda_1,\lambda_2)}{dx_1dx_2} = \frac{d^2\sigma_0}{dx_1dx_2}[1-\lambda_1\lambda_2-(\lambda_1-\lambda_2)A_{LR}]. \tag{23}$$

Here

$$\frac{d^2\sigma_0}{dx_1dx_2} = \frac{\alpha_{\text{QED}}^2 N_C}{12\pi s}g_{Hff}^2\left\{G_A\frac{x_H^2}{(1-x_1)(1-x_2)} - 2[g_V^2(e)+g_A^2(e)]g_A^2(f)(1+x_H)X_Z^2\right\} \tag{24}$$

– the differential cross section of this process in the case of unpolarized particles, and

$$A_{LR} = \frac{G_D x_H^2 - 4g_V(e)g_A(e)\,g_A^2(f)(1+x_H)(1-x_1)(1-x_2)X_Z^2}{G_D x_H^2 - 2[g_V^2(e)+g_A^2(e)]\,g_A^2(f)(1+x_H)(1-x_1)(1-x_2)X_Z^2} \tag{25}$$

– left-right spin asymmetry due to the longitudinal polarization of the electron and the designation introduced

$$G_D = 2Q_eQ_f\,g_A(e)g_V(f)X_Z + 2g_V(e)g_A(e)[g_V^2(f)+g_A^2(f)]X_Z^2 \ .$$

The left-right spin asymmetry A_{LR} in the process $e^- + e^+ \to H + t + \bar{t}$ at $x_2 = 0.95$ approximately 17.6% and slightly increases with growth x_1, remaining almost constant. The same character is the left-right spin asymmetry in the process $e^- + e^+ \to H + \tau^- + \tau^+$. However, in this process, the left-right spin asymmetry is almost three times less than in the process $e^- + e^+ \to H + t + \bar{t}$.

Due to the weak interaction in the process under consideration, fermion and antifermion can be produced longitudinally polarized. Taking into account the longitudinal polarizations of the heavy fermion pair, the differential cross section integrated over the angles is:

$$\frac{d^2\sigma(h_1,h_2)}{dx_1dx_2}=\frac{1}{4}\cdot\frac{d^2\sigma_0}{dx_1dx_2}[1+h_1h_2+(h_1+h_2)P_f]. \quad (26)$$

Here

$$P_f=\{Q_eQ_fg_V(e)g_A(e)X_Z+[g_V^2(e)+g_A^2(e)]\,g_V(f)g_A(f)X_Z^2\}\times$$

$$\times\{(1-x_1)[x_Hx_2c_{23}+3(1-x_1)]-(1-x_2)[x_Hx_1(c_{23}c_{21}-s_{23}s_{21})+3(1-x_2)]\}\times. \quad (27)$$

$$\times\{G_Ax_H^2-2(1-x_1)(1-x_2)[g_V^2(e)+g_A^2(e)]\,g_A^2(f)(1+x_H)X_Z^2\}^{-1}$$

– degree of longitudinal polarization of the fermion or antifermion in the coordinate system IIIb.

In fig. 4 shows the dependence of the degree of longitudinal polarization t-quark in the process $e^-+e^+\to H+t+\bar{t}$ on the variable x_1 at a fixed scaling energy $x_2=0.9$ and $x_2=0.95$. From the graphs it follows, that with increasing scaling energy x_1 the degree of longitudinal polarization decreases monotically. However, at a fixed quark energy x_1 with an increase in the antiquark energy x_2, the magnitude of the degree of longitudinal polarization increases.

Interestingly, the degree of longitudinal polarization of the fermion $P_f(x_1,x_2)$ changes its sign when replacing $x_1\leftrightarrow x_2$: $P_f(x_1,x_2)=-P_f(x_2,x_1)$.

Note that the degree of longitudinal polarization t-quark has already been measured by the ATLAS detector in the process of hadron production of a pair $t\bar{t}$ at the Large Hadron Collider [38].

Now consider the particle distribution over the angles θ and φ. In this case, the annihilation cross section of a transversely polarized electron-positron pair, integrated over the azimuth angle χ, has the form

$$\frac{d^4\sigma(\eta_1,\eta_2)}{d\varphi d(\cos\theta)dx_1dx_2}=\frac{d^4\sigma_0}{d\varphi d(\cos\theta)dx_1dx_2}[1+A_\perp\eta_1\eta_2\cos 2\varphi], \quad (28)$$

where

$$\frac{d^4\sigma_0}{d\varphi d(\cos\theta)dx_1dx_2}=\frac{\alpha_{\mathrm{QED}}^2N_C}{128\pi^2s}g_{Hff}^2G_A(\sigma_1+2\sigma_3)(1+\alpha_0)(1+\alpha_1\cos^2\theta) \quad (29)$$

– differential cross section of this process in the case of unpolarized particles,

$$A_\perp=\frac{\beta_1\sin^2\theta}{1+\beta_1\cos^2\theta}\cdot\frac{F_B}{F_A} \quad (30)$$

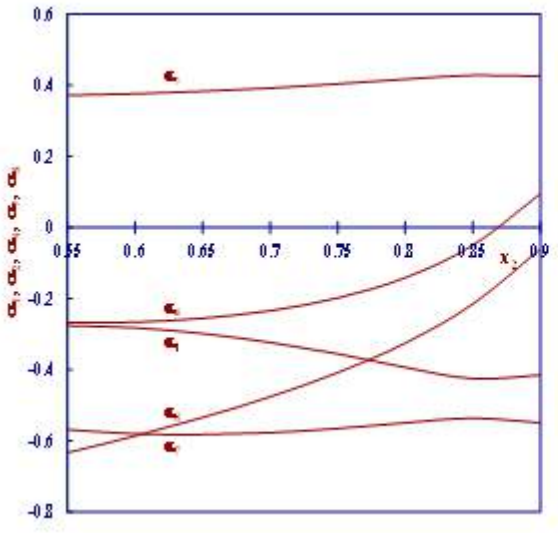

Fig. 3. Dependence of the angular distribution coefficients on the energy x_2 in the reaction $e^-e^+\to Ht\bar{t}$ for $x_1=0.9$, $\sqrt{s}$ = 1 TeV, M_Z = 91.1875 GeV, m_t = 173.2 GeV.

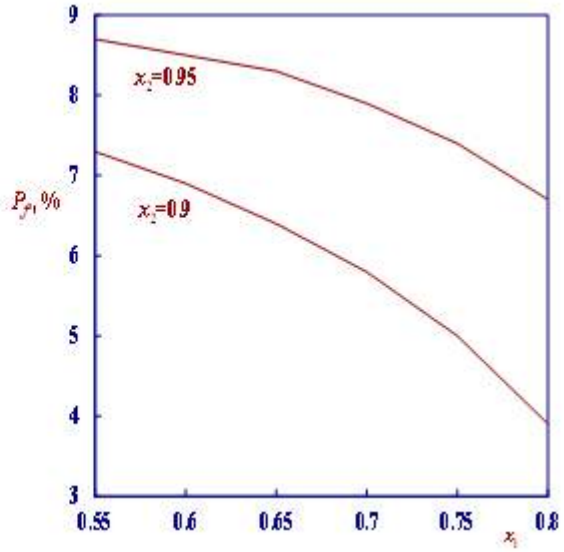

Fig. 4. The degree of longitudinal polarization in the process $e^-e^+\to Ht\bar{t}$ as a function of the energy x_1 for different x_2.

– transverse spin asymmetry due to transverse polarizations of the electron-positron pair. The notation is entered here

$$\beta_1 = \frac{\sigma_1 - 2\sigma_3}{\sigma_1 + 2\sigma_3},$$

$$F_A = G_A \frac{x_H^2}{2(1-x_1)(1-x_2)} - [g_V^2(e) + g_A^2(e)] g_A^2(f)(1+x_H) X_Z^2, \tag{31}$$

$$F_B = \frac{x_H^2}{2(1-x_1)(1-x_2)} \{Q_e^2 Q_f^2 + 2Q_e Q_f X_Z g_V(e) g_V(f) + X_Z^2 [g_V^2(e) - g_A^2(e)] \times$$
$$\times [g_V^2(f) + g_A^2(f)]\} - X_Z^2 [g_V^2(e) - g_A^2(e)] g_A^2(f)(1+x_H),$$

In fig. 5 shows the angular dependence of the transverse spin asymmetry (30) in the process $e^- + e^+ \to H + t + \bar{t}$ at $x_1 = 0.95$ and in the three values of the variable $x_2 = 0.55$, 0.6, and 0.65. As the angle θ increases, the transverse spin asymmetry increases and reaches a maximum at an angle of $\theta = 90°$, and then the asymmetry decreases and vanishes at the end of the angular spectrum. The growth of the variable x_2 leads to a decrease in the transverse spin asymmetry.

5. THE DISTRIBUTION OF PARTICLES IN A VARIABLE T

Dalitz distribution density on variable x_1 and x_2 has a simple and compact form, which coincides with the result of [32]

$$\frac{d^2\sigma_0}{dx_1 dx_2} = \frac{\alpha_{\text{QED}}^2 N_C}{12\pi s} g_{Hff}^2 \left\{ G_A \left[2 + \frac{1-x_1}{1-x_2} + \frac{1-x_2}{1-x_1} \right] - 2[g_V^2(e) + g_A^2(e)] g_A^2(f)(1+x_H) X_Z^2 \right\} \tag{32}$$

In fig. 6 shows the dependence of the cross section (32) in the process $e^- + e^+ \to H + t + \bar{t}$ on the variable x_2 with fixed $x_1 = 0.9$ and $x_1 = 0.95$ .With increasing scaling energy x_2, the cross section monotonously decreases, and a decrease in the variable x_1 also leads to a decrease in the cross section.

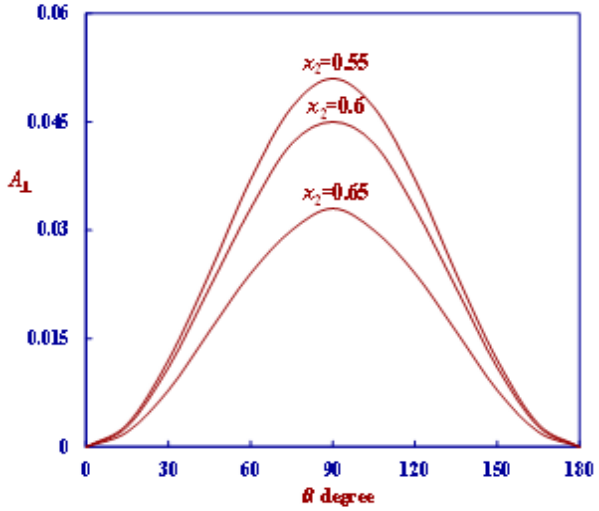

Fig. 5. The transverse spin asymmetry in the process $e^- e^+ \to Ht\bar{t}$ as a function of the angle θ at $x_1 = 0.95$ for different x_2.

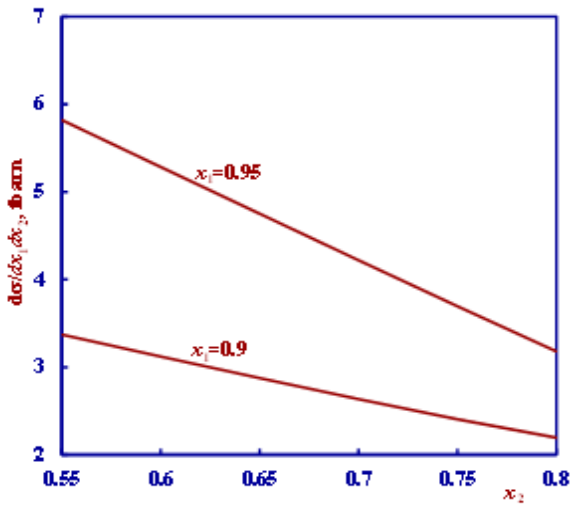

Fig. 6. Dependence of the cross section of the process $e^- e^+ \to Ht\bar{t}$ on the energy x_2 for different x_1 and $\sqrt{s}$ = 1 TeV, M_Z = 91.1875 GeV, m_t = 173.2 GeV.

We introduce new variables $T = T_1 = \max(x_1, x_2, x_H)$, T_2 and T_3 so that inequalities $T = T_1 \geq T_2 \geq T_3 = 2 - T - T_2$ are satisfied. We direct the axis Z along the momentum of the most energetic particle and integrate the section in a variable T_2 with a fixed T one. Then we get the following results:

1) at $x_H = T$ and $x_1 = T_2$ (or $x_2 = T_2$)

$$\frac{d\sigma}{dT} = \frac{\alpha_{\text{QED}}^2 N_C}{12\pi s} g_{Hff}^2 \times \left\{ G_A T \ln\left(\frac{1-T}{T}\right) - \frac{1}{4}[g_V^2(e) + g_A^2(e)] g_A^2(f)(1+x_H) X_Z^2 (12-5T)(3T-2) \right\} \quad ; \tag{33}$$

2) at $x_1 = T$ and $x_2 = T_2$ (or at $x_2 = T$ and $x_1 = T_2$):

$$\frac{d\sigma}{dT} = \frac{\alpha_{\text{QED}}^2 N_C}{12\pi s} g_{Hff}^2 \left\{ G_A \left[\frac{(3T-2)(6-5T)}{2(1-T)} - (1-T)\ln\left(\frac{2T-1}{1-T}\right) \right] - \right.$$
$$\left. - \frac{1}{4}[g_V^2(e) + g_A^2(e)] g_A^2(f) X_Z^2 (12-5T)(3T-2) \right\}; \quad (34)$$

3) at $x_1 = T$ and $x_H = T_2$ (or at $x_2 = T$ and $x_H = T_2$)

$$\frac{d\sigma}{dT} = \frac{\alpha_{\text{QED}}^2 N_C}{12\pi s} g_{Hff}^2 \left\{ G_A \left[\frac{(3T-2)(2-T)}{2(1-T)} + (1-T)\ln\left(\frac{2T-1}{1-T}\right) \right] - \right.$$
$$\left. - \frac{1}{4}[g_V^2(e) + g_A^2(e)] g_A^2(f) X_Z^2 (12-5T)(3T-2) \right\}. \quad (35)$$

By adding the contributions to the cross section of individual regions of the Dalitz diagram, we obtain the cross section characterizing the distribution of the most energetic particle in a variable T:

$$\frac{d\sigma}{dT} = \frac{\alpha_{\text{QED}}^2 N_C}{12\pi s} g_{Hff}^2 \left\{ G_A \left[\frac{(3T-2)(4-3T)}{(1-T)} + T\ln\left(\frac{1-T}{T}\right) \right] - \right.$$
$$\left. - \frac{3}{4}[g_V^2(e) + g_A^2(e)] g_A^2(f) X_Z^2 (12-5T)(3T-2) \right\}. \quad (36)$$

In fig. 7 illustrates the dependence of the cross section of the reaction $e^- + e^+ \to H + t + \bar{t}$ on the variable T for $\sqrt{s} = 1$ TeV and $m_t = 173.2$ GeV. Growth of the variable T from 0.725 to 0.9 leads to a monotonic increase in the cross section from 0.252 fbarn to 4.529 fbarn.

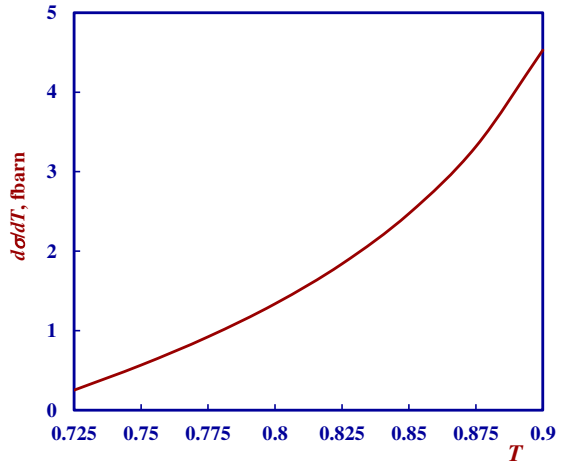

Fig. 7. Dependence of the cross section of the process $e^-e^+ \to Ht\bar{t}$ on the variable T for the $\sqrt{s}$ = 1 TeV, M_Z = 91.1875 GeV, m_t = 173.2 GeV.

Note that an experimental study of the reaction $e^- + e^+ \to H + t + \bar{t}$ is of great interest, since it allows you to accurately measure the coupling constant g_{Htt}. Although the Higgs boson coupling constants with gauge bosons g_{HWW}, g_{HZZ} are measurable in the LHC, the direct measurement of the constant g_{Htt} is difficult. Consequently, the study of the Higgs boson radiation process by top quarks in high-energy electron-positron collisions represents a certain interest.

CONCLUSION

Thus, we discussed the process of the associated production of the Higgs boson H and a longitudinally polarized heavy fermion pair in the annihilation of an arbitrarily polarized electron-positron pair $e^- + e^+ \to (\gamma^*; Z^*) \to H + f + \bar{f}$. An analytical expression of the differential cross section of the process is obtained, the features of the cross section behavior, angular correlations of particles, left-right spin asymmetry A_{LR}, the degree of longitudinal polarization of the fermion P_f, and transverse spin asymmetry $A_\perp$ are investigated. The results of the calculations are illustrated with graphs. The possibility of experimental measurement of the coupling constant g_{Htt} is discussed.

APPENDIX

Here we give the expressions for the correlation functions in the coordinate systems IIa, IIb, IIIa and IIIb.

1) In systems IIa and IIb:

$$\sigma_1 = \frac{2x_H^2}{(1-x_1)(1-x_2)}(2-s_{13}^2),$$

$$\sigma_2 = \frac{x_H^2}{(1-x_1)(1-x_2)} \cdot s_{13}^2,$$

$$\sigma_3 = \frac{2x_H^2}{(1-x_1)(1-x_2)}(1-c_{13}^2),$$

$$\sigma_4 = \mp \frac{2x_H^2}{(1-x_1)(1-x_2)} \cdot s_{13}c_{13}$$

$$\sigma_7 = 2x_H \left[\frac{x_2}{1-x_2}(c_{13}-c_{12}) + \frac{x_1}{1-x_1}(1-c_{13}) \right]$$

$$\sigma_8 = \mp x_H\left[-\frac{x_2}{1-x_2}(s_{13}+s_{12})+\frac{x_1}{1-x_1}s_{13}\right]$$

$$\sigma_1' = -4(1+x_H)\,(2-s_{13}^2), \qquad \sigma_2' = -2(1+x_H)\,s_{13}^2,$$

$$\sigma_3' = -4(1+x_H)\,(1-c_{13}^2), \quad \sigma_4' = \pm 4(1+x_H)\cdot s_{13}c_{13};$$

2) In systems IIIa and IIIb:

$$\sigma_1 = \frac{2x_H^2}{(1-x_1)(1-x_2)}\cdot(2-s_{23}^2),$$

$$\sigma_2 = \frac{x_H^2}{(1-x_1)(1-x_2)}\cdot s_{23}^2,$$

$$\sigma_3 = \frac{2x_H^2}{(1-x_1)(1-x_2)}\cdot(1-c_{23}^2),$$

$$\sigma_4 = \mp\frac{2x_H^2}{(1-x_1)(1-x_2)}\cdot s_{23}c_{23}$$

$$\sigma_7 = 2x_H\left[\frac{x_2}{1-x_2}(c_{23}-1)-\frac{x_1}{1-x_1}(c_{23}-c_{21})\right],$$

$$\sigma_8 = \mp x_H\left[\frac{x_2}{1-x_2}s_{23}-\frac{x_1}{1-x_1}(s_{23}+s_{21})\right],$$

$$\sigma_1' = -4(1+x_H)\,(2-s_{23}^2), \qquad \sigma_2' = -2(1+x_H)\,s_{23}^2,$$

$$\sigma_3' = -4(1+x_H)\,(1-c_{23}^2), \quad \sigma_4' = \pm 4(1+x_H)\cdot s_{23}c_{23}.$$

The upper sign corresponds to systems IIa and IIIa, and the lower IIb and IIIb.

---

[1] *A. Djouadi.* The Anatomy of Electro-Weak Symmetry Breaking. Tome I: The Higgs boson in the Standard Model. arXiv: hep-ph/0503172v2, 2005; DOI: 10.1016 /j.physrep. 2007.10.004.

[2] *S.K. Abdullayev*. Standard model, properties of leptons and quarks. Baku, 2017, 276p. (in Azerbaijan).

[3] *V.M. Emelyanov*. Standard Model and its extensions, Moscow, FIZMATLIT, 2007, 584p. (in Russian).

[4] *P. Langacker.* The Standard Model and Beyond. CRS Press, 2010, 635p. DOI: http://dx.doi.org/10.1063/1.36182.

[5] *C. Partignani et al.* (Particle Data Group) Chin. Phys., 2016, C 40, p. 100001.

[6] *G. Aad* et al. ATLAS Collaboration Phys. Lett., 2012, B 716, p.1.

[7] *S. Chatrchyan et al.* CMS Collaboration Phys. Letters, 2012, B 716, p. 30.

[8] *V.A.Rubakov*. To the creation of new particle with Higgs boson properties on Big Hadron Collider, UFN, 2012, vol.182, №10, pp.1017-1025.

[9] *A.V. Lanev*. CMS collaboration results: Higgs boson and search of new physics UFN, 2014, vol. 184, № 9, pp. 996-1004.

[10] *D.I. Kazakov*. Higgs boson is discovered: what else? UFN, 2014, vol. 184, № 9, pp. 1004-1017.

[11] *F. Englert, R. Brout.* Broken Symmetry and the mass of gauge vector Mesons Phys. Rev. Letters, 1964, V.13, №9, p.321.

[12] *P.W. Higgs.* Broken Symmetries and the Masses of gauge Bosons. Phys. Rev. Letters, 1964, V.13, №16, p.508.

[13] *P.W. Higgs.* Spontaneous Symmetry Breakdown without Massless Bosons Phys. Rev., V. 145, 1966, p. 1156-1163.

[14] *G.S. Guralnik, C.R. Hagen, T.W. Kibble.* Global Conservation Laws and Massless Particles Phys. Rev. Lett., 1964, V. 13, pp. 585-587.

[15] *S.K. Abdullayev, M.Sh. Gojayev, F.A. Saddigh.* Decay Channels of the Standard Higgs boson Moscow University Physics Bulletin, 2017, v.72, №4. P. 329-339; VMU, series 3: Physics, Astronomy, 2017, №4, p.3-11.

[16] *S.K. Abdullayev, M.Sh. Gojayev, N.A. Nasibova.* Production of a scalar boson and fermion pair in arbitrarily polarized e^-e^+-beams. Russian Physics Journal, 2018, v.61, №1, p.94-101.

[17] *S.K. Abdullayev* and *M.Sh. Gojayev.* The Higgs bosons production in arbitrary polarized electron-positron colliding beams UZFF, 2018, No 1, pp. 1810101-1-10.

[18] *P. Nath.* Higgs physics and supersymmetry Int. J. Mod. Phys. A., 2012, V.27, No28, pp.123029.

[19] *R.K. Barman* et. al. Current status of MSSM Higgs sector with LHC 13 TeV data. arXiv: 1608.02573v3 [hep-ph] 23 May 2017.

[20] *Z. Hioki, T. Konishi, K. Ohkuma.* Studying possible CP-violating Higgs couplings through top-quark pair productions at muon colliders Journal of High Energy Physics, 2017, V. 7, No 07. arXiv: 0706.4346v2 [hep-ph], 2017.

[21] M. Greco. On the study of the Higgs properties at a muon collider Mod. Phys. Lett., A30, 2015, No. 39, pp. 1530031 [arXiv:1503.05046].

[22] *S. Jadach, R.A. Kycia.* Lineshape of the Higgs boson in future lepton colliders Phys. Lett. B755, 2016, pp.58-63 [arXiv:1509.02406].

[23] *K. Peters.* Prospects for beyond Standart Model Higgs Boson searches at future LHC runs and other machines. arXiv: 1701.05124v2 [hep-ex] 21 Feb 20.

[24] *S.K. Abdullayev, L.A. Agamaliyeva, M.Sh. Gocayev, F. Saddigh.* Investigation of Higgs boson formation in lepton-antilepton collisions GESJ: Physics, 2015, №1(13), p.36-55.

[25] *S.K. Abdullayev, L.A. Agamaliyeva, M.Sh. Gocayev.* Investigation of Higgs boson formation in deep-inelastic lepton-antilepton dispersion GESJ: Physics,2015, №2(14), p.28-40.

[26] *S.K. Abdullayev, M.Sh. Gojayev* and *F.A. Saddigh.* AJP. Fizika. Baku, V. XXI 2015, №2, pp.17-22.

[27] *S.K. Abdullayev, M.Sh. Gojayev and N.E. Nesibova*. AJP. Fizika, 2017, V. XXII, № 3, p.45-52.

[28] *S.K. Abdullayev, M.Sh. Gojayev*. Production and decay of Higgs bosons in muon collieders / X International conference «Modern trends in Physics», Baku, 2017, 20-22 April.

[29] LHC Higgs Cross Section Working Group Collaboration, de Florian D. et al. «Handbook of LHC Higgs Gross Sections: 4. Deciphering the nature of the Higgs Sector» arXiv: 1610.07922v1[hep-ph], 2016.

[30] *V.D. Shiltsev*. High-energy particle colliders: the past 20 years, the next 20 years, and the distant future UFN, 2012, V. 182, No 10, pp.1033-1046.

[31] *K.J.F. Gaemers, G.J. Gounaris.* Phys. Lett., 1978, B 77, No 4, pp. 379-382.

[32] *A. Djouadi J. Kalinovski, P.M. Zerwas.* Two- and Three-Body Decay Modes of SUSY Higgs Particles. arXiv: hep-ph / 9511342V1, 16 Nov, 1995.

[33] *A. Djouadi.* The Anatomy of Electro-Weak Symmetry Breaking. Tome II: arXiv: hep-ph/0503173v2, 2003;
DOI: 10.1016/j.physrep.2007.10.005

[34] *S.K. Abdullayev, M.Sh. Gojayev*. AJP: Fizika, XXIV (4), 11, 2018.

[35] *S.K. Abdullayev M.Sh. Gojayev*. Associated Production of a Higgs Boson and Heavy Fermion Pair in e^-e^+-collisions Moscow University Physics Bulletin, 2019, V. 74, No 1, pp.24-32.

[36] *S.K. Abdullaev, A.I. Mukhtarov*. Superstring Z'-boson in e^-e^+-annihilation PEPAN, 1995, V. 26, No 5, pp. 527-552.

[37] *S.K. Abdullaev, A.I. Mukhtarov*. Physics of Atomic Nuclei, 1997, V. 60, No 11, pp.1901-1919.

[38] *S.F.Hamilton*. CERN-THESIS-2014-008, 2014, p. 279.

Received: 22.10.2019